AD_____

Award Number: W81XWH-10-1-0326

TITLE: Tracked Ultrasound Elastography for Neo-adjuvant Chemotherapy Monitoring

PRINCIPAL INVESTIGATOR: Pezhman, Foroughi, Ph.D.

CONTRACTING ORGANIZATION: Johns Hopkins University
Baltimore MD 21218

REPORT DATE: May 2011

TYPE OF REPORT: Annual Summary

PREPARED FOR: U.S. Army Medical Research and Materiel Command
Fort Detrick, Maryland 21702-5012

REPORT DOCUMENTATION PAGE

Form Approved
OMB No. 0704-0188

1. REPORT DATE	2. REPORT TYPE	3. DATES COVERED
May 2011	Annual Summary	1 May 2010 – 30 April 2011

4. TITLE AND SUBTITLE

Tracked Ultrasound Elastography for Neo-adjuvant Chemotherapy Monitoring

5a. CONTRACT NUMBER

5b. GRANT NUMBER
W81XWH-10-1-0326

5c. PROGRAM ELEMENT NUMBER

6. AUTHOR(S)

Pezhman, Foroughi

E-Mail: pezhman@cs.jhu.edu

5d. PROJECT NUMBER

5e. TASK NUMBER

5f. WORK UNIT NUMBER

7. PERFORMING ORGANIZATION NAME(S) AND ADDRESS(ES)

Johns Hopkins University
Baltimore MD 21218

8. PERFORMING ORGANIZATION REPORT NUMBER

9. SPONSORING / MONITORING AGENCY NAME(S) AND ADDRESS(ES)
U.S. Army Medical Research and Materiel Command
Fort Detrick, Maryland 21702-5012

10. SPONSOR/MONITOR'S ACRONYM(S)

11. SPONSOR/MONITOR'S REPORT NUMBER(S)

12. DISTRIBUTION / AVAILABILITY STATEMENT
Approved for Public Release; Distribution Unlimited

13. SUPPLEMENTARY NOTES

14. ABSTRACT

We are building a novel monitoring system based on ultrasound elastography which detects the changes in size, shape, and stiffness of tumors in patients receiving neoadjuvant chemotherapy. This system will be used for in-vivo assessment of chemo-sensitivity and early detection of drug resistance. We have developed an ultrasound elastography technique which decreases the dependency of the quality of the images to the expertise of the operator and generates consistent and high-quality strain imaging. It employs information from an external tracker to select frame pairs with minimal lateral and out-of-plane motion, and at the same time, controls the compression rate. We have also devised a customized stereo camera system to accurately reconstruct the surface of the breast for tumor registration and localization. This system projects multiple light patterns on the surface of the breast and resolves for the depth. Experiment on breast phantoms, elastography phantoms, and pig's liver have been carried out to validate the performance of these methods.

15. SUBJECT TERMS
Neoadjuvant chemotherapy, Monitoring, Ultrasound, Elastography, Tracking, Surface reconstruction, Strain, Tumor stiffness, Electromagnetic tracker

16. SECURITY CLASSIFICATION OF:			17. LIMITATION OF ABSTRACT	18. NUMBER OF PAGES	19a. NAME OF RESPONSIBLE PERSON
a. REPORT	b. ABSTRACT	c. THIS PAGE			19b. TELEPHONE NUMBER *(include area code)*
U	U	U	UU	18	USAMRMC

Table of Contents

	Page
Introduction……..…….. 1	
Body…….. 2	
Key Research Accomplishments…….…….. 6	
Reportable Outcomes…… 6	
Conclusion…… 6	
References……. 7	
Appendices…… 8	

INTRODUCTION:

We are developing new imaging techniques based on ultrasound elastography for monitoring the changes in size, shape and stiffness of tumors in patients receiving Neoadjuvant chemotherapy (NAC). NAC is often administered to women with operable stage II or III breast cancer with an operable tumor. It may shrink the size of the tumor and enhance breast conservation. Success of NAC depends on assessment of chemo-sensitivity and early detection of the response of the tumor to the administered drug. However, the clinical tools used to monitor the response of cancer to NAC are less than ideal due to imprecision, high cost, and accessibility issues.

Ultrasound systems on the other hand are widely accessible, cost-effective, and portable. Therefore, an ultrasound-based monitoring system could be used to regularly screen the changes in the tumor during the procedure and help with timely detection of drug resistance. We have been developing such a system, and our main achievements towards this goal can be categorized into four parts.

First, we built the interface to connect a new 3D ultrasound probe ideal for elastography to our ultrasound machine. This involved both hardware and software development. The hardware is composed of probe wiring and connection to the ultrasound machine, a motor controller, and a digitizer to record the position of the probe. The software sends commands to the transducer and controls its motion. There are also functions available to read raw data from the probe, save the data, reconstruct 3D volumes, and send the data over a local network. This task had been completed in collaboration with the MUSiiC laboratory at the Laboratory for Computational Sensing and Robotics, Johns Hopkins University [1].

Second, we developed a customized stereo camera system with structured light to reconstruct the surface of the patient's breast. This task was not directly sought in the original statement of work. The 3D surface reconstruction system largely aids the deformable registration and localization of the tumor over time. The idea is to reconstruct the 3D surface of the breast each time prior to data collection from the patient. This surface is registered to the pre-treatment CT scan of the patient which will provide a base-line for comparison. This system is capable of mapping the surface with sub-millimeter accuracy. The structured light in this system compensates for the lack of features on the surface of the skin.

Third, we further developed our tracked ultrasound elastography (TrUE) to achieve better accuracy, increased robustness to noise, and higher image quality [2]. We now exploit the image content in addition to the tracking information to refine the displacement field. We have also incorporated a new strain estimation method that analytically solves for motion field [3]. Furthermore, we fuse multiple images to increase the signal-to-noise ratio (SNR) of the output image.

Finally, we have carried out a series of experiments on a breast phantom, an elastography phantom, and pig's liver. The breast phantom was employed to test our structured light stereo system and our tracked elastography method. A more controlled experiment was possible with the elastography phantom since the exact properties of this phantom are known. The ex-vivo and in-vivo experiment with the pig's liver provides a more challenging environment close to clinical setups with the associated uncertainties. The in-vivo experiment is especially challenging due to the internal motions such as blood flow

and breathing. The collected data from these experiments are only partially analyzed, and complete results will be published in near future.
I have also expanded my knowledge about various aspects of breast cancer, medical imaging, and elastography. As a part of my training, I regularly attended weekly meeting, seminars, and a journal club.

BODY:

Task 1: Breast cancer training

My clinical and engineering mentors have been very helpful by both tutoring me and directing me to the relevant articles, books, and online resources. In this period, I have been studying the various subjects on breast cancer such as the types, the risk factors, and the epidemiology of breast cancer. I also learned more about treatment options available for different stages and types of breast cancer especially NAC. Through regular meetings, we discussed research issues, applicability and practicality of our proposed techniques, the problems that need to be resolved and potential solutions. I closely followed the advancements in ultrasound and elastography by attending a weekly journal club and presenting recent publications. I also broadened my scientific knowledge by attending seminars and lab meetings. Although the subjects of these seminars may not have been directly related to my research, but they exposed me to new ideas and approaches that could be useful in my own research. The topics included computer integrated diagnoses and intervention, medical image analysis, image processing, ultrasound, and physics of medical imaging.

Task 2: System integration and registration

2a. 3D reconstruction

3D reconstruction refers to creating volumetric data from 2D images for which spatial information is available. The images may be b-mode ultrasound or estimated strain maps. We have implemented a C++ code that reads the input images and their corresponding spatial transformations, applies probe calibration to the transformations, and reconstructs a 3D volume. Two methods have been implemented for reconstruction. Either a value for each voxel in the volume is south by finding the nearest pixels in all images, or the pixels of the images are scanned and merged into the nearest voxel [4]. Interpolation is necessary for both approaches. We have also developed visualization software with tools for manipulating and reslicing the volumes using visualization toolkit (VTK) [5]. These programs have been integrated into our data collection and synchronization software.

2b. 3D probe interface and volume stitching

We have a new high-frequency linear transducer capable of moving its elements in precise linear steps (micrometer resolution) to construct a cubic ultrasound volume (Figure 1). This transducer has multiple advantages over the traditional wobbler and the linear array probes. The linear motion of this transducer makes it suitable for

volumetric elastography since the spacing between the lines remains constant, and there are fewer variations in the size of the resolution cell. Also, uniform force can be applied to the tissue due to the flat surface of the probe. This is an important feature for elastography which helps in constructing a uniform image. The volume is also large compared to linear arrays.

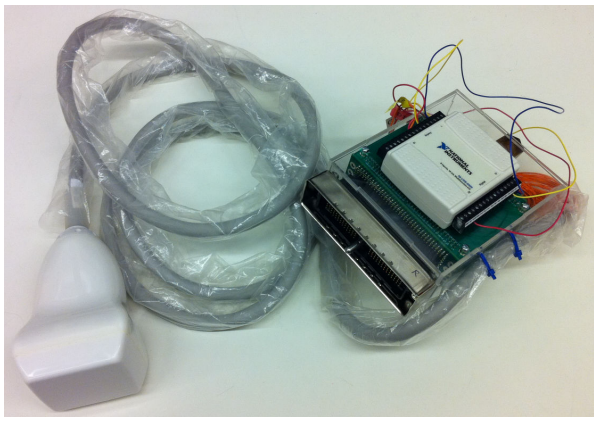

Figure 1: The 3D ultrasound transducer and our interface board.

We built an interface for this probe shown in Figure 1. This interface is required for acquiring ultrasound data from the probe and consists of both hardware and software components. The hardware has three parts. There is a connector to attach the probe to the ultrasound machine. The wiring for the connector is made possible by 6 PCB boards each of which has 6 metal layers. Three of these layers are used for shielding and suppressing the noise. The motor controller has a separate board and controls the step motion of the elements inside the probe. The last component is a digitizer that converts the position feedback from the controller unit into digital signals (Figure 2). The controller and the digitizer are connected to the ultrasound machine via USB port. The power for the controller is provided by a separate power supply.

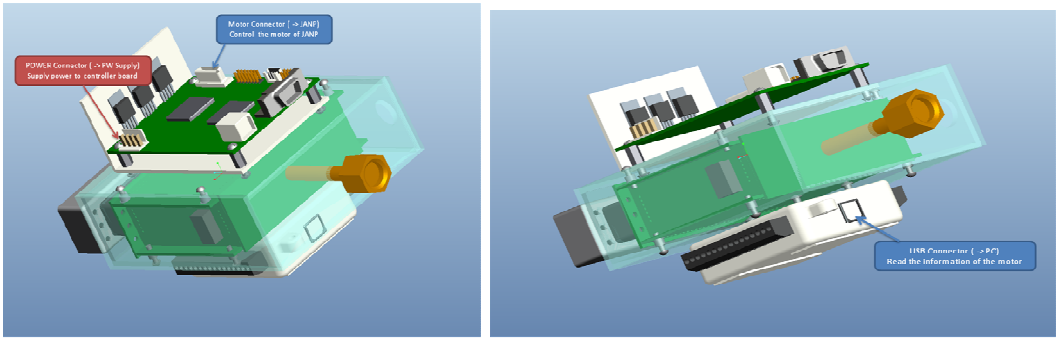

Figure 2: The hardware interface for the 3D transducer

The software component detects the probe and controls the imaging parameters as well as the motion of the motor of the transducer. By sending commands to the controller, it adjusts the speed, step size, and direction of the motor. This software is a part of a toolkit developed in MUSiiC lab [1] referred to as MUSiiC-Toolkit [6]. We also have a protocol to send the images (both 2D and 3D) over a local network to a

third party computer for further processing based on openIGTlink [7]. This will facilitate extended computational power for real-time processing.

2c. Deformable registration

We have revised the original plan for registration and localization of the tumors. In the original plan, we intended to directly register the 3D scans of the tumor together, which is a difficult task and may require additional supervision for failure detection. It also does not capture the shifts in tumor position with respect to the breast anatomy. In the new plan, we employ a stereo camera system to capture the 3D surface of the breast. This surface is then registered to the surface extracted from the pre-treatment CT scan. We will use a newly introduced point set registration method called "coherent point drift" [8] for deformable registration. The advantage is that the CT will provide a base-line for all ultrasound scans. The registration will be more reliable and it will be easier to track the changes in shape, size, position, and stiffness of the tumor since the images taken during the course of treatment are aligned with respect to the patient's breast.

To this end, we have developed a customized stereo system to reconstruct the 3D surface of breast. This system is specifically designed for breast imaging and consists of two cameras and a projector (see Figure 3).

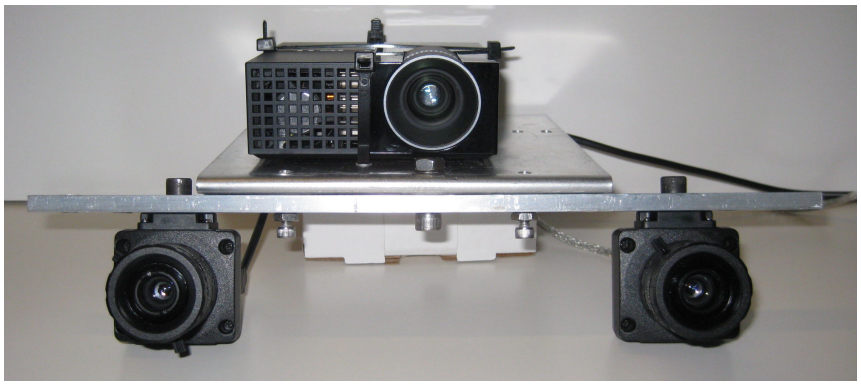

Figure 3: Structured light stereo system

This device is mounted on a tripod facing down toward the breast. The projector projects several light patterns on the breast while the two cameras records the images of the breast (Figure 4 left). The structure light creates virtual features on the featureless surface of the breast. The pictures from individual patterns are stacked together creating a vector of several RGB values for each pixel. Having the camera calibration, the corresponding points in the images are triangulated to solve for the depth map (Figure 4 right). For this purpose, we have developed a C++ code as a "mex" function that can be called within MATLAB. This code is optimized for speed and can reliably generate 3D depth maps since several images with different light patterns are used. The patterns are specifically designed for this application. With the current implementation, only a few seconds are required to reconstruct the 3D map of the surface with sub-millimeter accuracy.

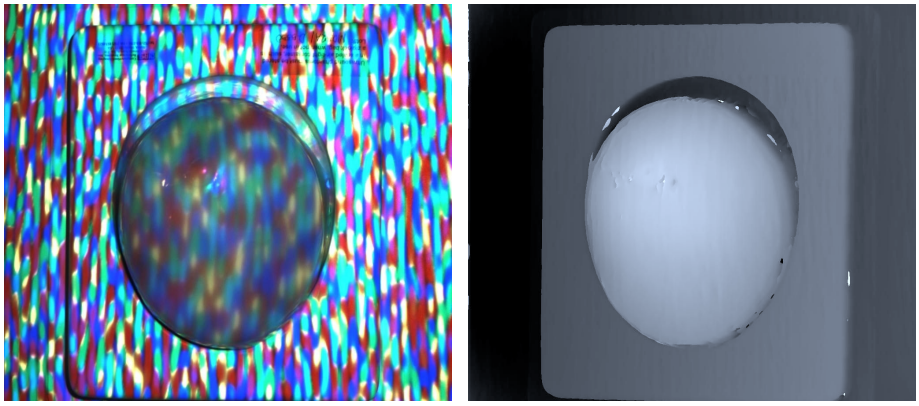

Figure 4: The left image shows the breast phantom under structured light, and the image on the right shows the reconstructed depth map.

Task 3. Development of 2D and 3D TrUE

3a. Fusion of DP-based USEI and TrUE framework

Tracked ultrasound elastography (TrUE) is a frame selection technique which seaches for the best frame pairs that could be used for elastography [2]. In TrUE, we exploited the tracking data to enhance the quality of the elasticity images in two ways. First, having the tracking information, multiple pairs of images containing optimal hand motion are selected. The optimum value for lateral and out-of-plane motions is zero, and the optimum axial motion is selected by the user. Second, the strain images obtained from these pairs are fused together based on the location of each strain image to improve image quality. We now exploit the image content in addition to the tracking information to refine the displacement field. The details of this method can be found in the attached appendix, Section 2.

In original implementation of TrUE, we used a normalized cross correlation (NCC) based technique to estimate the displacement map. NCC is slow and prone to errors due to decorrelation. In our new implementation, we have incorporated a new strain estimation method that is fast and shown to be robust to noise and outliers [3]. Our initial evaluations are very promising. A complete analysis of the performance of this technique is underway.

Task 4. Clinical data collection, analysis, and validation

4a. Breast phantom evaluation

We carried out experiments on breast phantoms and pig liver to evaluate our developed imaging techniques. The results of these experiments are reported in the appendix, Section 3. We are processing the in-vivo data taken from pig liver. The advantage of experimenting with live tissue is that the internal motions due to breathing and blood flow are not omitted. These experiments also help us detect possible glitches and improve our system for fast data collection. Based on these experiments we will be working on a data acquisition protocol with breast cancer patients.

KEY RESEARCH ACCOMPLISHMENTS

1. Software development for data collection, volume reconstruction, and visualization.
2. Interfacing a new 3D ultrasound transducer for elastography.
3. Building a stereo camera system with structured light optimized for breast imaging.
4. Enhancing the performance our frame selection technique by using image content, fusing multiple images together, and incorporating an advanced displacement estimation technique.
5. Evaluating the developed techniques on breast phantoms and pig's liver.

REPORTABLE OUTCOMES

- Pezhman Foroughi, Hassan Rivaz, Ioana N. Fleming, Gregory D. Hager, and Emad M. Boctor, "Tracked ultrasound elastography (TrUE)" *Medical image computing and computer-assisted intervention*, Part II, pp. 9—16, 2010

CONCLUSION

The proposed monitoring system for NAC is aimed at personalizing the treatment for patients undergoing NAC procedure by early detection of drug resistance and assessment of chemo-sensitivity. In this period, we have been developing the components of our monitoring system and creating the necessary testbed for evaluation of the effectiveness of it. The new 3D probe is now ready for data acquisition and the structured light stereo system can create high resolution 3D maps of the surface of the breast. This map will be used for registration of datasets taken in different time intervals. The preliminary results of our tracked ultrasound elastography method show that it can produce consistent and high-quality strain images. In the next step, we will be integrating all these components into one system. We will also be conducting more experiments and analysis including in-vivo animal experiments to test the resistance of TrUE to internal motions such as the ones induced by heart-beat and respiration. Finally, we will move toward a complete clinical trial by first seeking IRB and other necessary approvals. Although our specific target is breast cancer, there are several other clinical applications which may benefit from the techniques developed in this work.

REFERENCES

[1] https://musiic.lcsr.jhu.edu/Research

[2] P. Foroughi, H. Rivaz, I. N. Fleming, G. D. Hager, and E. M. Boctor, "Tracked ultrasound elastography (TrUE)" *Medical image computing and computer-assisted intervention*, Part II, pp. 9—16, 2010

[3] H. Rivaz, E. M. Boctor, M. A. Choti, and G. D. Hager, "Real-Time Regularized Ultrasound Elastography" *IEEE Transactions on Medical Imaging*, vol. 30(4), pp. 928-945, 2011

[4] R. Rohling, A. Gee, L. Berman, and G. Treece, "Radial Basis Function Interpolation for Freehand 3D Ultrasound" *Proceedings of the 16th International Conference on Information Processing in Medical Imaging*, pp. 478-483, 1999

[5] http://www.vtk.org/

[6] https://musiic.lcsr.jhu.edu/Research/MUSiiC_Toolkit

[7] J. Tokuda, et. al, "OpenIGTLink: an open network protocol for image-guided therapy environment" *The International Journal of Medical Robotics and Computer Assisted Surgery*, vol. 5(4), pp. 423-434, 2009

[8] A. Myronenko, and X. Song, "Point set registration: Coherent Point Drift" *IEEE Transactions on Pattern Analysis and Machine Intelligence*, vol. 32, pp. 2262-2275, 2010

Tracked Ultrasound Elastography (TrUE)

Pezhman Foroughi[1], Hassan Rivaz[1], Ioana N. Fleming[1],
Gregory D. Hager[1], and Emad M. Boctor[1,2]

[1] Dept. of Computer Science, Johns Hopkins University, Baltimore, MD, USA
[2] Dept. of Radiation Oncology, Johns Hopkins University, Baltimore, MD, USA

Abstract. This paper presents a robust framework for freehand ultrasound elastography to cope with uncertainties of freehand palpation using the information from an external tracker. In order to improve the quality of the elasticity images, the proposed method selects a few image pairs such that in each pair the lateral and out-of-plane motions are minimized. It controls the strain rate by choosing the axial motion to be close to a given optimum value. The tracking data also enables fusing multiple strain images that are taken roughly from the same location. This method can be adopted for various trackers and strain estimation algorithms. In this work, we show the results for two tracking systems of electromagnetic (EM) and optical tracker. Using phantom and *ex-vivo* animal experiments, we show that the proposed techniques significantly improve the elasticity images and reduce the dependency to the hand motion of user.

Keywords: Ultrasound, Elastography, Elasticity, Tracking, Strain.

1 Introduction

Ultrasound elastography is an emerging medical imaging modality which involves imaging the mechanical properties of tissue and has numerous clinical applications. Among many variations of ultrasound elastography [1], our work focuses on real-time static elastography, a well-known technique that applies quasi-static compression of tissue and simultaneously images it with ultrasound. Within many techniques proposed for static elastography, we focus on freehand palpation elasticity imaging which involves deforming the tissue by simply pressing the ultrasound probe against it. Freehand ultrasound elastography has shown great potential in clinical applications especially for diagnosis and screening of breast lesions [2]. The application of elastography is not limited to breast, and other applications such as diagnosis of prostate cancer, monitoring ablation and deep vein thrombosis have also been studied.

Despite the reports on success of elastography, yet it has not become a part of any routine clinical application. The main reason is that elastography is highly qualitative and user-dependent. The best result is achieved when the user compresses and decompresses the tissue uniformly in the axial direction with the proper hand motion. It is difficult to control the compression rate as it is governed by the hand motion and the frame rate of RF data. Also, small lateral

T. Jiang et al. (Eds.): MICCAI 2010, Part II, LNCS 6362, pp. 9–16, 2010.

or out-of-plane motions can compromise the quality of images. However, it is difficult to induce pure axial motion with freehand compression. Sophisticated algorithms can only partially address the problem by compensating for in-plane motions and applying smoothness constraints. The images are also hard to interpret, and artifacts –caused by failure of the strain estimation algorithm or poor hand motion– may be mistaken for lesions inside the soft tissue. Developing an elastography technique that is not affected by poor hand motion and other sources of signal decorrelation will pave the way for wide-spread clinical use of elastography.

To improve the reliability, quality metrics such as persistence in strain images have been developed [3,4]. This quality indicator is calculated for each image and provided to the user as feedback. Persistence is also used to merge multiple elasticity images together [3]. To measure the persistence, strain is computed for two pairs of echo frames, and the resulting images are correlated. Although these techniques offers a major advantage, there remains several limitations. First, the strain has to be estimated before the calculation of the quality metric. With typical ultrasound settings, the frame rate can reach more than 30 Hz. For subsequent frames, an efficient implementation of this image-based metric might cope with this rate. Nonetheless, the task will be extremely difficult to try all the combinations in a series of frames. Moreover, the quality metric will not be able to provide feedback to the user whether he/she should adjust the palpation in certain direction. Also, there would be minimal control over the strain rate.

The ultrasound probe is often tracked in navigation/guidance systems to provide spatial information, to form freehand 3D ultrasound, or to facilitate multimodality registration. In this work, we exploit the tracking data to enhance the quality of the elasticity images. We use the tracking data to select multiple image pairs that contain the optimum deformation for the elastography algorithm. The optimum value for lateral and out-of-plane motions is zero, and the optimum axial motion is determined by the specific elastography algorithm used, which is Normalized Cross-Correlation (NCC) in this work. Next, we fuse the strain images obtained from the multiple image pairs together based on the location of each strain image to improve image quality. We assume that the ultrasound data is 2D. Nonetheless similar techniques proposed here could be extended to 3D ultrasound.

2 Methodology

Consider a sequence of RF data collected during the palpation of tissue using a tracked transducer. We have previously shown that it is possible to synchronize the RF frames with the tracking information relying only on the same data collected during palpation [5]. From synchronization, the tracking information is interpolated at the incident time of each frame. The input to our algorithm is then a series of RF frames along with their corresponding transformation.

First, we need to define a distance function between two frames of RF data. For this purpose, we use a model of image decorrelation in presence of out-of-plane and lateral motion. RF signal is often modeled as the collective response

of scatterers randomly distributed within the resolution cell of the ultrasound [6,7]. Each scatterer is assumed to have an amplitude governed by the shape of the resolution cell and a phase which is distributed from 0 to π uniformly at random. Considering a Gaussian shape for the resolution cell Prager *et. al* [8] calculated the correlation as a function of out-of-plane motion to be $exp(-\frac{\delta^2}{2\sigma^2})$. δ and σ denote the displacement and the width of the resolution cell respectively. Although this function is only valid for fully developed speckle, it provides a convenient estimate of correlation. It should be noted that in [8], the displacement is estimated from correlation, whereas here, we intend to define an energy function based on displacement. Extending this formula to both out-of-plane and lateral displacements, we define our energy function, $E(x, z)$, as follows:

$$E(D_x, D_z) = exp(-K_x \cdot D_x^2 - K_z \cdot D_z^2), \tag{1}$$

where D_x and D_z represent the displacement in out-of-plane and lateral directions. E does not depend on axial motion (D_y) since displacement in axial direction is necessary for strain estimation. K_x and K_z determine the sensitivity to a certain direction. In order to be able to use this function, we need a component-wise metric representing the distance of two frames given their homogeneous transformations. The first step is to compute the relative transformation between them. Suppose $a = [a_x\ a_y\ a_z]^T$ is the axis-angle representation of the relative rotation, and $t = [t_x\, t_y\, t_z]^T$ is the relative translation. Assuming a small rotation, the relative displacement of a point, $P = [x\, y\, 0]^T$, will be $d = a \times P + t$. We then define the distance vector of two frames, $D = [D_x\, D_y\, D_z]^T$, as the RMS of the components of d for all the points in the region of interest (ROI):

$$\begin{aligned}
D_x &= sqrt\{\ \frac{1}{(y_2 - y_1)} \int_{y_1}^{y_2} (-a_z \cdot y + t_x)^2 dy\ \}, \\
D_y &= sqrt\{\ \frac{1}{(x_2 - x_1)} \int_{x_1}^{x_2} (a_z \cdot x + t_y)^2 dx\ \}, \\
D_z &= sqrt\{\ \frac{1}{(y_2 - y_1)(x_2 - x_1)} \int_{x_1}^{x_2} \int_{y_1}^{y_2} (a_x \cdot y - a_y \cdot x + t_z)^2 dy dx\ \},
\end{aligned} \tag{2}$$

where $sqrt\{.\}$ returns the root. Here, ROI is assumed to be rectangular and determined by x_1, x_2, y_1, and y_2. The vector D provides a measure of distance for each direction separately. We use this vector in Equation (1) which gives us an estimate of "pseudo-correlation" over the ROI.

The data goes through four stages of processing to create a single high-quality strain image. In the first step, few images are selected from the data series that are approximately collected from one cross-section of tissue with minimal lateral and out-of-plane motion. To this end, the energy function of each frame is computed with respect to all other frames in the sequence. Then, the total energy is found for each frame as the sum of the energies of the M closest frames, where closeness implies higher energy, and M is the maximum number of frames to be selected. Then, the frame with the highest total energy (the center frame)

is identified, and the M closest frames to the center frame including itself are selected. Additionally, the frames that have E of less than 0.5 with respect to the center frame are disqualified. This is applied to ensure lower number of frames are chosen when M frames from one cross-section are not available.

In the next stage, the program evaluates all possible combination of frame pairs for elastography. For M frames, there will be $\binom{M}{2} = M(M-1)/2$ pair combinations which will be compared using a slightly modified version of E. Since the pairs are directly compared, it suffices to minimize the exponent of Equation (1) in order to maximize E. We also add a term for axial motion that penalizes compressions that are higher than an optimum compression value, t_{opt}. Hence, a "cost function", $C1$, is defined as follows:

$$C1(D) = K_x \cdot D_x^2 + K_y \cdot \tilde{D_y}^2 + K_z \cdot D_z^2, \quad \tilde{D_y} = \begin{cases} D_y - t_{opt}, & |D_y - t_{opt}| > 0 \\ 0, & |D_y - t_{opt}| \leq 0 \end{cases} \tag{3}$$

where t_{opt} implies the optimal strain, which can be theoretically defined as described in [9]. Here, t_{opt} is set depending on the robustness of the elasticity estimation algorithm. Its value might be within the range of the resolution of the tracker. Therefore, at this stage we do not assign a penalty for the compressions less than t_{opt}. If the compression is close to zero, the contrast of the reconstructed image degrades. The program filters the pairs with low compression in the next stage using image content. Similar to the first part, a maximum number of frames with lowest cost are selected provided that the cost is lower than a threshold. The threshold is not strict to ensure acceptable pairs are not filtered.

The final pairs are selected by recovering the global lateral motion and compression by matching the two RF frames in each pair. The tracking information is used to initialize the search. For instance, the search range for compression is set to be from zero to the tracker reading in axial direction padded in both sides with the maximum error of the tracker. Given two frame I_1 and I_2, the amount of lateral motion a, and compression, b, is found by solving cross-correlation:

$$\arg\max_{a,b} \left\{ \sum_{x,y \in G} I_1(x,y) \cdot I_2(x+a, by) + I_1(x-a, -by) \cdot I_2(x,y) \right\}. \tag{4}$$

The RF data is normalized with standard variation and assumed to have zero mean. We employ two tricks which extensively increases the speed of search. First, we do not match the entire image to solve for these parameters. Instead, only pixels on a grid, G, are used as described by Equation (4). The two terms of Equation (4) ensures that the search remains reciprocal, which means switching the images only affects the sign of a and b. Second, a is recovered by matching only the top part of the two images while b is fixed to one. The reason is that the displacement due to compression is minimal in that region.

Having the global motions, the cost function is modified to penalize very low compressions:

$$C2(\widehat{D}) = K_x \cdot \widehat{D_x}^2 + K_y \cdot \frac{|\widehat{D_y} - t_{opt}|^3}{\widehat{D_y} + c} + K_z \cdot D_z^2, \tag{5}$$

where $\widehat{D_x}$ and $\widehat{D_y}$ are the global motions from Equation (4) converted to mm. c is a small number that limits the cost of zero compression. Finally, the pairs with the lowest cost are selected until a maximum number of frame pairs is reached or the minimum cost grows higher than the average cost.

The last step involves computing the strain for all the selected frame pairs. We have implemented normalized cross-correlation (NCC) [10] to recover the displacements and least squares estimation to calculate the strain. Before calculating strain, the global lateral motion and compression from the previous step are compensated in one image using cubic interpolation. This is known to reduce the error of strain estimation [11]. The final strain image, S_{final} is the weighted average of all the strains:

$$S_{final} = \frac{\sum_{i=1}^{m} w_i \cdot S_i}{\sum_{i=1}^{m} w_i}, \; w_i = \begin{cases} \frac{\rho_i}{1-\rho_i}, & \rho_i > 0.7 \\ 0, & otherwise \end{cases} \tag{6}$$

where ρ_i is the correlation coefficient for the ith pair after applying the displacements, and m is the number of pairs. Fusing the strains in this fashion is acceptable since the algorithm only allows for compressions that are close to a predetermined amount optimal for strain estimation.

3 Experiments and Results

We acquired ultrasound data using a SONOLINE Antares$^{\text{TM}}$ ultrasound system (Siemens Medical Solutions USA, Inc.) with a high-frequency ultrasound transducer (VF10-5) at center frequency of 6-8 MHz. We accessed RF through the Axius Direct$^{\text{TM}}$ Ultrasound Research Interface provided by Siemens. Our custom data acquisition program was connected to this interface to send the command for capturing RF data. At the same time, the program collected tracking information from either a "Polaris" optical tracker (Northern Digital Inc., Waterloo, Canada) with passive markers or the "medSAFE" EM tracker (Ascension Tech. Corp.).

RF data and tracking information was captured from a breast phantom containing a harder lesion (CIRS elastography phantom, Norfolk, VA) and *ex-vivo* pig liver. Alginate was injected to the liver to mark a part of liver, and then, that area was ablated. The users were asked to palpate the tissue over the hard lesion in the breast phantom and the ablated lesion in the pig liver while data was being collected. Between 100 to 138 RF frames were acquired with the rate of about 30 frames per second.

The first set of data was captured by an experienced user from the breast phantom. Figure 1(a) shows the translation components of hand motion with respect to the first frame. The axial motion is dominant and there is only a gradual drift in the lateral and elevational directions. Figure 1(b) depicts the high-quality strain image resulting from the TrUE algorithm.

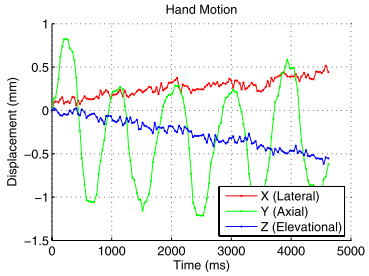

(a) Freehand palpation

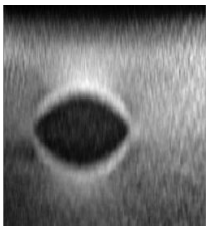

(b) Strain image (TrUE)

Fig. 1. (a) shows the translation of probe w.r.t. the first image. Proper hand motion is applied as the axial compression is dominant. (b) is the output of our proposed algorithm.

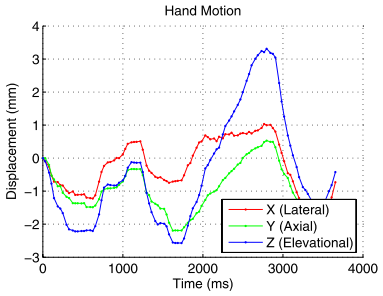

(a) Poor palpation with EM tacking

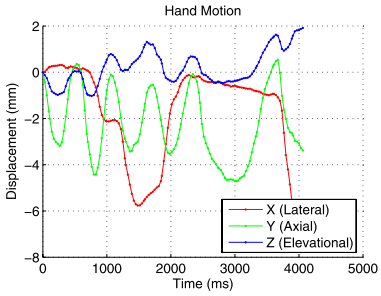

(b) Poor palpation with optical tracking

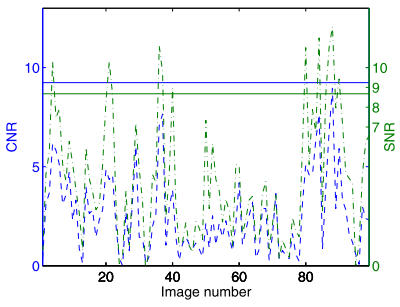

(c) Consecutive vs. TrUE

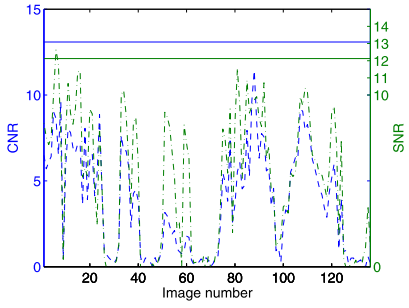

(d) Consecutive vs. TrUE

Fig. 2. Two cases of improper motions are shown where the hand motion suffers from large lateral and elevational components evident in relative translations. The results of case 1 with EM tacker is shown on the left column, and the results of case 2 with optical tracker is shown on the right column.

Applying a compression similar to the one shown in Figure 1(a) is a difficult task for novice or even intermediate users. This is especially the case where axial compression does not translate into a simple up and down motion. Ultrasound gel creates a slippery surface that makes the palpation prone to out-of-plane motion. Two case are shown in Figure 2, where one is tracked with the EM tracker and the other one with the optical tracker. In Figure 2(a) the hand motion contains a large amount of out-of-plane motion, whereas, in Figure 2(b), the user has moved the probe laterally. In both cases, the TrUE algorithm generates reliable results. Figures 2 (c) and (d) show the contrast-to-noise ratio (CNR) and signal-to-noise ratio (SNR) of the strain image. The CNR and SNR value are computed from:

$$\text{CNR} = \sqrt{\frac{2(\bar{s}_b - \bar{s}_t)^2}{\sigma_b^2 + \sigma_t^2}}, \quad \text{SNR} = \frac{\bar{s}}{\sigma}, \tag{7}$$

where $\bar{s}$ and σ denote the mean and standard deviation of intensities. The $_t$ or $_b$ subscripts show that the computation is only for the target or the background region, respectively. The SNR and CNR for computing the strain from consecutive frames (the dashed curve) is compared to the SNR and CNR of the strain image from the proposed method (solid line). Using consecutive frames is the standard method of elastography in ultrasound machines. Almost in all cases the TrUE algorithm outperforms the consecutive frames by a large margin.

Although the SNR and CNR provide quantitative measures to compare the strain images, they do not directly reflect the visual quality of strain. In Figure 3, we show results of elastography using our frame selection technique as well as four other strain images calculated from consecutive frames. The Figure shows the effects of improper compression in consecutive frames in the strain image. At the same time our algorithm provides a single reliable strain.

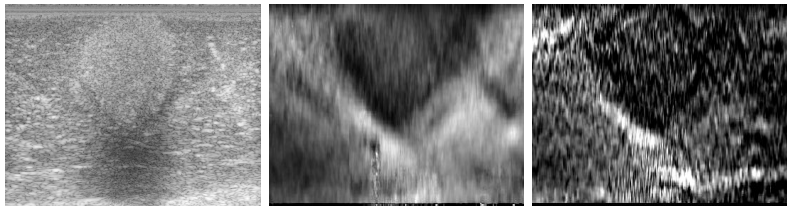

(a) B-mode (b) TrUE (c) 1&2

(d) 2&3 (e) 3&4 (f) 4&5

Fig. 3. Comparison of the strain from TrUE vs. consecutive frames for *ex-vivo* pig liver

4 Discussion

We presented a method of ultrasound elastography which is robust to the quality of the hand motion of the user. Using the information from an external tracker, it automatically selects multiple frame pairs with a specific compression and minimal undesired motions. Our approach does not take into account the tissue motion from other sources such as breathing or patient motion. However, these types of motions are not normally problematic since they occur with a slower pace compared to hand motion.

Our experiments shows that even when the transducer has severe lateral or out-of-plane motions, the algorithm still manages to produce good results. The multi-stage frame selection and careful image fusion makes the TrUE method less sensitive to tacker accuracy and robust to strain estimation failures.

We are planning to use the proposed method in a breast cancer study. For this purpose, we will be implementing our MATLAB code in C. The strain estimation which is still the bottleneck of our approach will be executed in GPU allowing for the use of sophisticated algorithms.

Acknowledgments. Pezhman Foroughi, Hassan Rivaz, and Ioana Fleming are supported by the U.S. Department of Defense pre-doctoral fellowship program.

References

1. Ophir, J., Alam, S., Garra, B., Kallel, F., Konofagou, E., Krouskop, T., Varghese, T.: Elastography: ultrasonic estimation and imaging of the elastic properties of tissues. Annu. Rev. Biomed. Eng. 213, 203–233 (1999)
2. Garra, B., et al.: Elastography of breast lesions: initial clinical results. Radiology 202, 79–86 (1997)
3. Lindop, J.E., Treece, G.M., Gee, A.H., Prager, R.W.: An intelligent interface for freehand strain imaging. Ultrasound Med. Biol. 34, 1117–1128 (2008)
4. Jiang, J., Hall, T.J., Sommer, A.M.: A novel strain formation algorithm for ultrasonic strain imaging. In: IEEE Ultrasonics Symposium, pp. 1282–1285 (2006)
5. Foroughi, P., Hager, G., Boctor, E.: Robust elasticity imaging using external tracker. In: IEEE Int. Symp. Biomed. Imag., pp. 209–212 (2009)
6. Wagner, R., Smith, S., Sandrik, J., Lopez, H.: Statistics of Speckle in Ultrasound B-Scans. IEEE Trans. Sonics and Ultrasonics 17(3), 251–268 (1983)
7. Shankar, P.: A general statistical model for ultrasonic backscattering from tissues. IEEE Trans. Ultrason. Ferroelectr. Freq. Control 47(3), 727–736 (2000)
8. Prager, R., et al.: Sensorless freehand 3-d ultrasound using regression of the echo intensity. Ultrasound Med. Biol. 29, 437–446 (2003)
9. Varghese, T., Ophir, J.: A theoretical framework for performance characterization of elastography: the strain filter. IEEE Transactions on Ultrasonics, Ferroelectrics and Frequency Control 44, 164–172 (1997)
10. Céspedes, I., Huang, Y., Ophir, J., Spratt, S.: Methods for estimation of subsample time delays of digitized echo signals. Ultrasound Imaging 17(2), 142–171 (1995)
11. Varghese, T., Ophir, J.: Performance optimization in elastography: Multicompression with temporal stretching. IEEE Transactions on Ultrasonics, Ferroelectrics and Frequency Control 18(22), 193–214 (1996)